

## Supplemental information

Realizing  $\text{Li}_7\text{La}_3\text{Zr}_2\text{O}_{12}$  garnet with high  $\text{Li}^+$  conductivity and dense microstructure by Ga/Nb dual substitution for lithium solid-state battery applications

Weijie Lan<sup>a</sup>, Hongyang Fan<sup>a</sup>, Vincent Wing-hei Lau<sup>b</sup>, Jiliang Zhang<sup>b</sup>, Jiafeng Zhang<sup>c</sup>,

Ruirui Zhao<sup>a1</sup>, Hongyu Chen<sup>a</sup>

- a. School of Chemistry, Engineering Research Center of MTEES (Ministry of Education), South China Normal University, Guangdong Guangzhou, 510006, P. R. China.
- b. Department of Energy and Materials Engineering, Dongguk University-Seoul, Seoul 04620, South Korea.
- c. School of Metallurgy and Environment, Central South University, Changsha Hunan, 410000, P. R. China.

---

<sup>1</sup> Corresponding Author. E-mail address: zhaoruirui@m.scnu.edu.cn

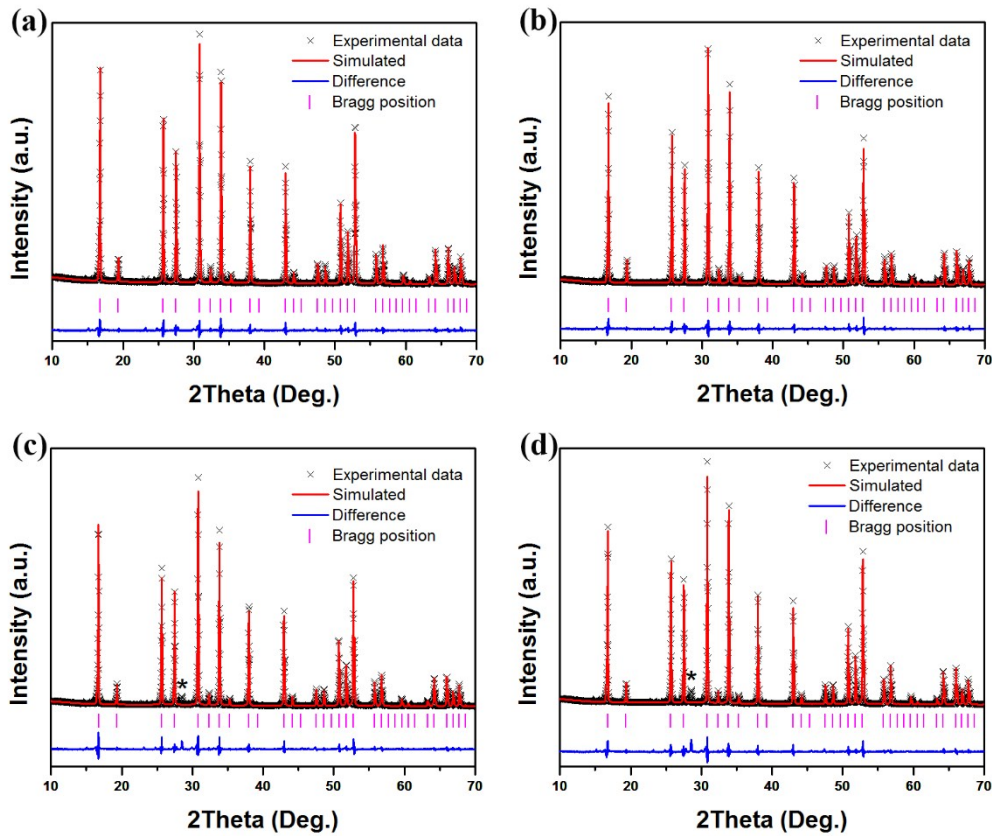


**Figure S1.** Rietveld refinements of the powder XRD data for the different LLZO pellets. (a) G15N20 ( $R_w = 5.12\%$ ), (b) G20N20 ( $R_w = 5.73\%$ ), (c) G25N20 ( $R_w = 4.42\%$ ) and (d) G30N20 ( $R_w = 4.78\%$ ). The asterisk \* marks the peak in (c) and in (d) an impurity phase ascribed to Ga-containing compound(s).

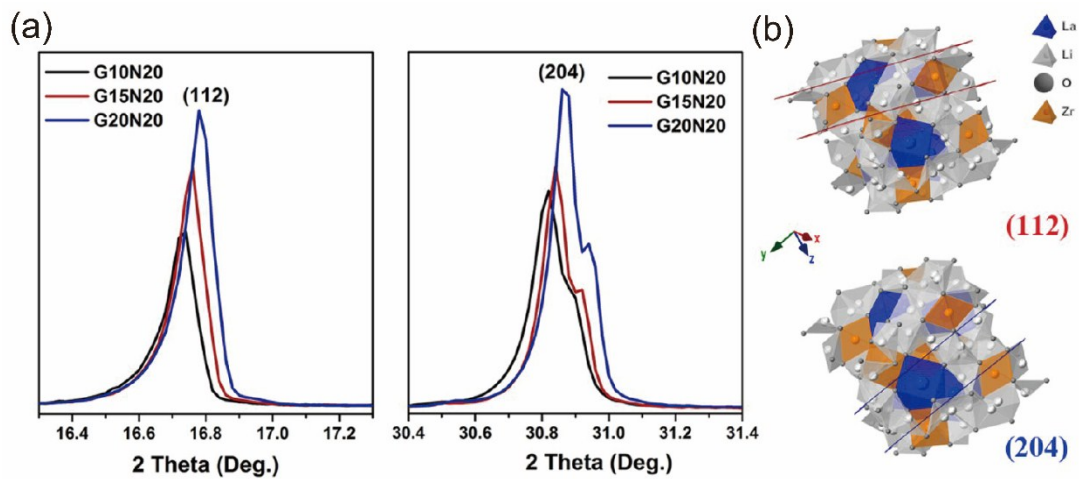


**Figure S2.** (a) The diffraction peaks of the (112) and (204) planes for G10N20, G15N20 and G20N20. (b) shows a visual representation of the crystal faces of (112) and (204).

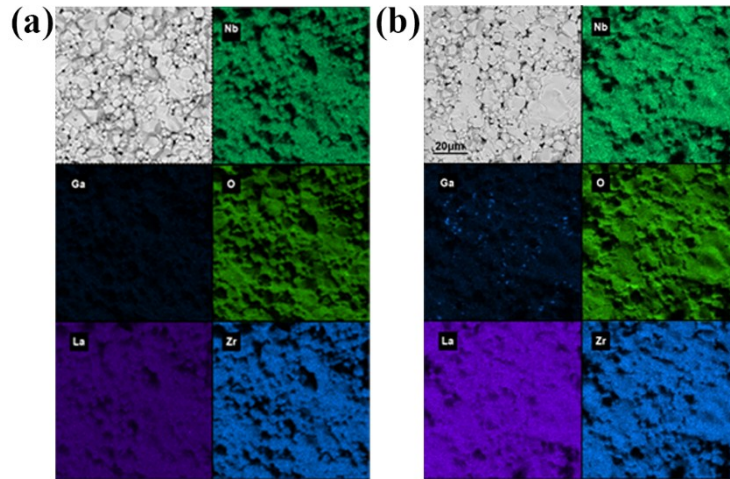


**Figure S3.** SEM corresponding EDS-mapping for (a) G10N20 and (b) G25N20

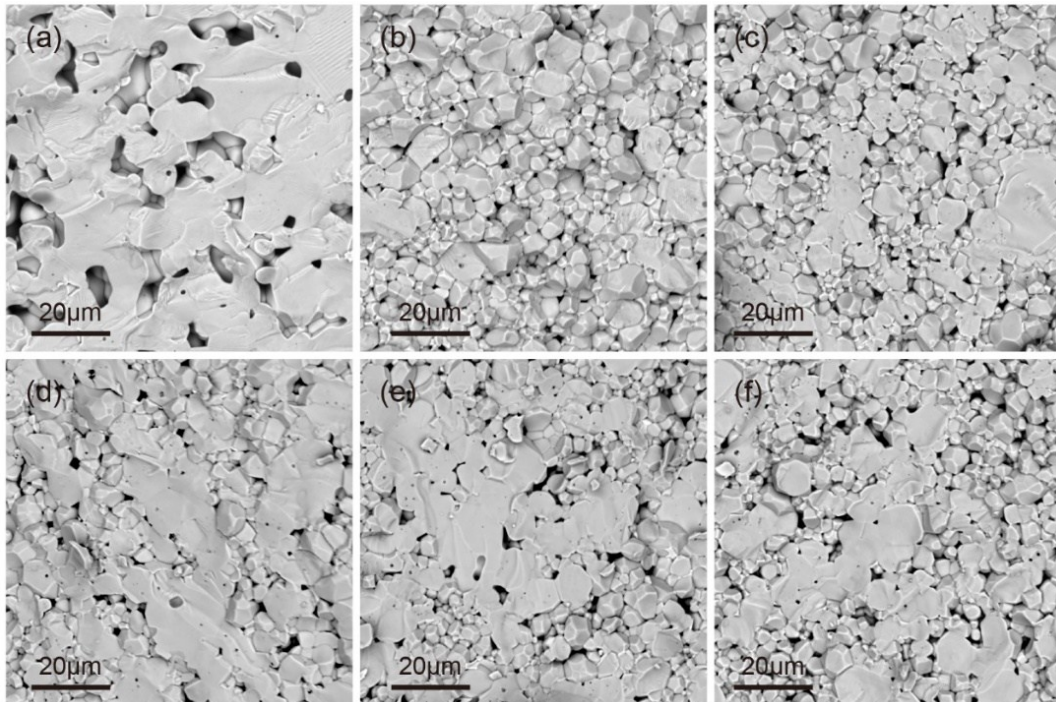


**Figure S4.** SEM images for the different LLZO pellets sintered at 1150 °C. (a) G00N20, (b) G10N20, (c) G15N20, (d) G20N20, (e) G25N20 and (f) G30N20

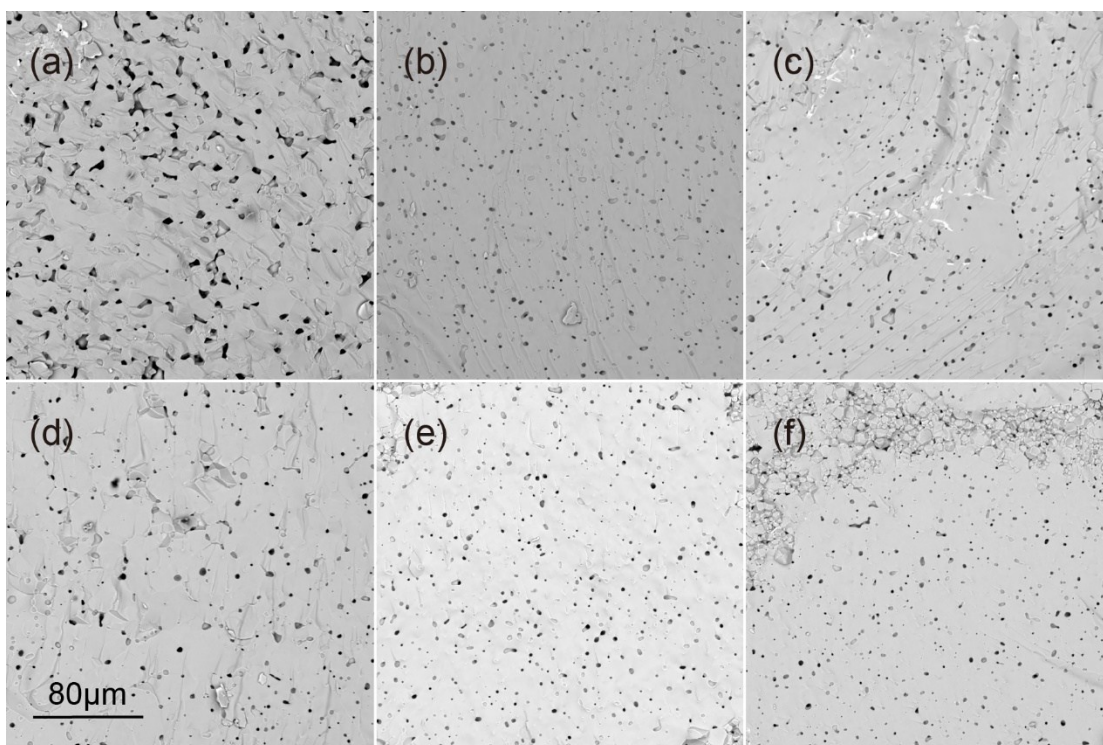


**Figure S5.** SEM images for the different LLZO pellets sintered at 1200 °C. (a) G00N20, (b) G10N20, (c) G15N20, (d) G20N20, (e) G25N20 and (f) G30N20

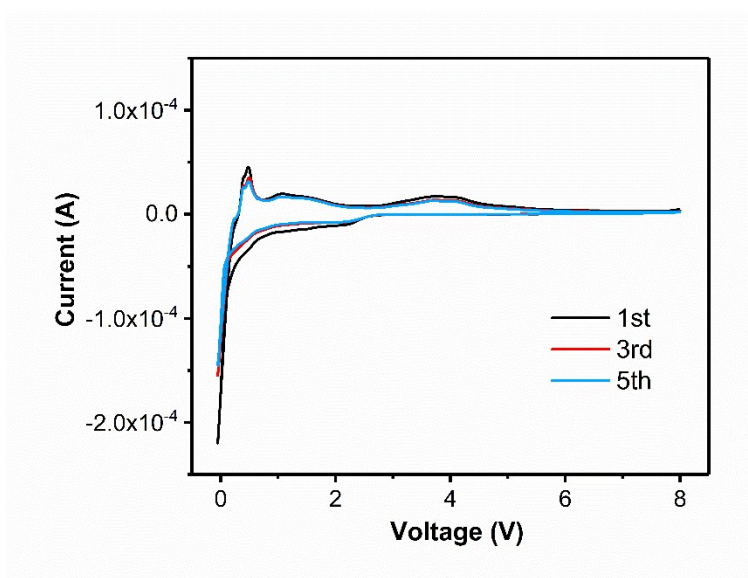


**Figure S6.** Cyclic voltammogram of the Li/G15N20/Au cell at  $1 \text{ mV s}^{-1}$ .

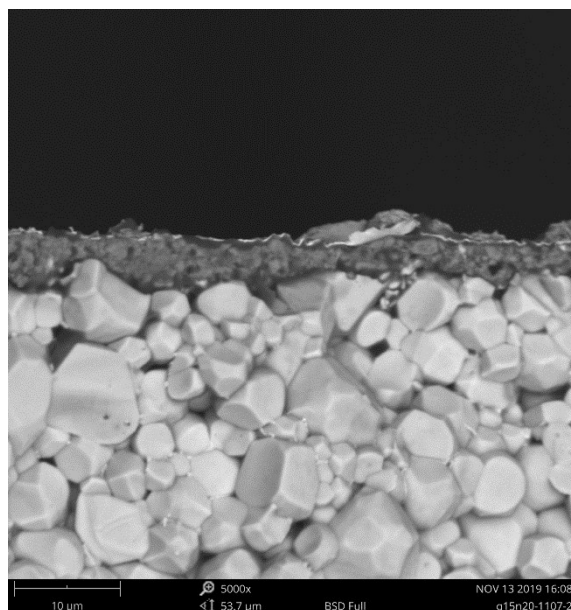


**Figure S7.** The SEM image of the interface of cathode and G15N20 in all solid-state battery

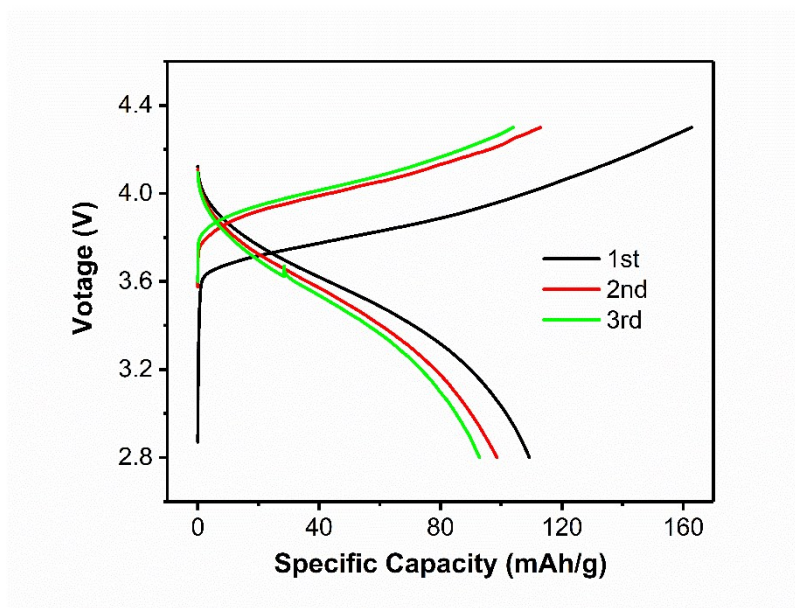


**Figure S8.** Charge/discharge profiles at 0.1C current for the first 3 cycles of Li/G15N20/NMC111 full cell (no liquid electrolyte).

**Table S1.** Chemical composition of  $\text{Li}_{6.8-3x}\text{Ga}_x\text{La}_3\text{Zr}_{1.8}\text{Nb}_{0.2}\text{O}_{12}$  samples by ICP-OES

	x	ICP-OES result				
		Li	La	Zr*	Nb	Ga
G00N20	0	6.725	3.177	1.8	0.198	--
G10N20	0.10	6.507	3.169	1.8	0.202	0.139
G15N20	0.15	6.313	3.161	1.8	0.199	0.180
G20N20	0.20	6.256	3.122	1.8	0.196	0.243
G25N20	0.25	6.175	3.155	1.8	0.197	0.286
G30N20	0.30	6.038	3.136	1.8	0.200	0.333

\*The quantity of all elements is normalized to that of Zr, which was fixed to 1.8.

**Table S2** The pellet density,  $\text{Li}^+$  conductivity as well as the activation energy for the different LLZO samples

	G00N20	G10N20	G15N20	G20N20	G25N20	G30N20
Relative density [%]	88.40	93.34	94.46	93.123	91.77	92.19
Total $\text{Li}^+$ conductivity [mS $\text{cm}^{-1}$ ]	0.357	0.675	0.739	0.720	0.504	0.372
Ea (eV)	0.4259	0.3603	0.3415	0.3443	0.3541	0.3555